DE GRUYTER OPEN

Acta Geophysica
vol. 64, no. 5, Oct. 2016, pp. 1655-1672
DOI: 10.1515/acgeo-2016-0035

Pareto Joint Inversion of 2D Magnetotelluric and Gravity Data – Towards Practical Applications

Katarzyna MIERNIK [1,2], Adrian BOGACZ [1,2], Adam KOZUBAL [1,2], Tomasz DANEK [1], and Marek WOJDYŁA [2]

[1] Department of Geoinformatics and Applied Computer Science, AGH – University of Science and Technology, Kraków, Poland; e-mail: danek9@geolog.agh.edu.pl
[2] Geopartner Ltd., Kraków, Poland

Abstract

In this paper, a Pareto inversion based global optimization approach, to obtain results of joint inversion of two types of geophysical data sets, is formulated. 2D magnetotelluric and gravity data were used for tests, but presented solution is flexible enough to be used for combination of any kind of two or more target functions, as long as misfits can be calculated and forward problems solved. To minimize dimensionality of the solution, space and introduce straightforward regularization Sharp Boundary Interface (SBI) method was applied. As a main optimization engine, Particle Swarm Optimization (PSO) was used. Synthetic examples based on a real geological model were used to test proposed approach and show its usefulness in practical applications.

Key words: Pareto joint inversion, Global Optimization, computer software, magnetotellurics, gravimetry.

1. INTRODUCTION

Proper reconstruction of a physical model on the basis of measured data is the final and the most critical part of any geophysical investigation. Without inversion, the gathered data are virtually useless from interpretational point of view

and cannot be used for creation of geological, petrophysical or reservoir model. In the case of analysis based only on one source of media information – namely of one geophysical field – details of this operation and most effective methods are relatively well know and studied (Sen and Stoffa 1995). Proper application of information gathered from many geophysical fields to create one geological model is a more challenging task. Inversion of different field observations can generate completely different parameter distribution geometries. It is mainly caused by the differences in methods' sensitivities and theirs spatial distribution over the model (Jegen *et al.* 2009). Moreover, physics of measured phenomena, observation scheme details, or even a methodology of inversion itself, can affect the shape of a final solution. A good example of the above-mentioned problems is comparison of results of classic singleobjective inversion of gravity and magnetotelluric (MT) data (*e.g.*, Abdelzaher *et al.* 2011) when the shapes of blurred object are usually incomparable and strongly dependent on used regularization (*e.g.*, Mehanee and Zhdanov 2002). Another independent problem with a comparison of different methods is the fact that the precision and accuracy of their results can significantly differ (DeStefano and Colombo 2006). In the case of classic singleobjective methods, their uncertainties are hard to compare, which can be critical for final quality evaluation of obtained petrophysical model parameters. One of the most natural methods of overcoming these problems is an application of joint inversion based on multiobjective target functions (MOP) (Vozoff and Jupp 1975), in which data from all methods are inverted simultaneously in the same numerical operation. In its most natural form, classic joint inversion methods have two important disadvantages. First of all, the definition of a proper, consistent target function is very difficult because of combining data of different dimensions and magnitudes. Usually this operation requires arbitrarily chosen weights to scale all objective function components to the same level, which makes it prone to subjective opinion of interpreter and not very practical for automatic methods. Moreover, combination of results of two or more different methods into one function can lead to dramatic increase of the number of model parameters, which requires strong regularization and causes significant, often unacceptable, raise in numerical intensity of computations. Secondly, classic joint inversion functions tend to generate highly multimodal solutions. This problem is typical for almost all geophysical methods but is even more critical in the case of multiobjective functions (Kozlovskaya *et al.* 2007).

In this paper a solution of these problems based on the combinations of few modern independent approaches is proposed. Target function definition and scaling problems are solved by Pareto inversion. This method is commonly used in economical studies and sometimes in geophysical inversion (Kozlovskaya *et al.* 2007). Pareto inversion scheme is based on simultaneous optimization of independent functions so the problems caused by combining target functions are completely eliminated. The problem of multimodality of solution can be

minimized by application of global optimization methods. Here Particle Swarm Optimization (PSO) method (Kennedy and Eberhart 1995, Poli *et al.* 2007) is applied. This relatively easy and straightforward method is very efficient in finding global minima in complex and deceptive functions. Its usefulness in geophysical problems was confirmed by many authors (*e.g.*, Danek *et al.* 2013, Fernandez Martinez *et al.* 2010). Target function dimensionality is limited by application of Sharp Boundary Interfaces (SBI) (Smith *et al.* 1999). In this method a geological model is described through a series of polygons or splines defined by nodal points. This method is sometimes used for stochastic geophysical inversion, *e.g.*, 2D magnetotellurics (Chen *et al.* 2012). Additionally in the presented solution some methods to prevent creation of non-geological solutions (*e.g.*, for crossing boundaries within one layer) are used. The main advantage of SBI is the fact that both reduction of problem dimensionality and regularization of the solution can be done in the same computational step.

2. JOINT INVERSION

Emergence and growing number of applications of joint inversion methods are a natural consequence of commonness of complex geophysical observation and interpretation methodology. The first method of this group was proposed in 1975 by Vozoff and Jupp (Vozoff and Jupp 1975), relatively late, taking under consideration that the beginning, of inversion itself dates back to the beginning of 19th century (Gauss 1809, Legendre 1805). At the beginning attempts were focused on inversion of single geophysical parameter, namely resistivity, using geophysical methods based on different physical backgrounds like MT and resistivity soundings. Later, progress resulted in methodology, in which geological model is created by combining information from methods, differing not only in the way of parameter observation but the parameter itself (Lines *et al.* 1988). The main goal of such operation is increased resolution in wide depth ranges. The classic example of an efficiency of this approach is a joint inversion of MT and gravity data over an area covered with high-resistivity extrusive basalt trapps (*e.g.*, Jegen *et al.* 2009). Combination of MT and gravity can give a solution with good resolution for both shallow and deep parts of the model.

In the simplest case of single target function, optimization misfit value ϕ is defined by:

$$\phi = \sum_{i=1}^{n} \frac{(dp_i - dm_i)^2}{\sigma_i^2}, \tag{1}$$

where n is a number of measurements, dp represents real data, dm are data returned by a tested model and σ represents data error. In a singleobjective case, application and statistical interpretation of this formula are straightforward. In multiobjective case, when adding more sections is necessary, two im-

portant problems arise. First of all, values returned by sums related to different methods are hard to compare and require proper, usually arbitrary, weighting. The second problem is a correct uncertainty analysis for two combined weighted objective functions. Elimination of arbitrary weighting of functions seems to be the critical step in creation of fully functional, robust and impartial method of joint inversion. Here application of Pareto inversion scheme as a solution of the above-mentioned problems is proposed.

3. PARETO METHOD

Historically, the theory of multiobjective optimization is connected with economical studies, because even a task as simple as cost minimal transport route calculation, requires simultaneous analysis of many factors and their mutual relations. Elimination of "manual" scaling is especially important for problems with fast changing conditions. Moreover, reducing the whole concept of multiobjective optimization to one scalar value of hypothetical target can lead to dramatic loss of information about details of multidimensional solution space. The idea of the Pareto inversion can be described starting from the definition of multiobjective minimum:

$$\min[f_1(x), f_2(x), \ldots, f_n(x)], x \in S\,, \tag{2}$$

where f_i represents target functions and S is a space of acceptable solutions.

Every solution proposition can be defined as:

$$C = \{y \in R^n : y = f(x) : x \in S\}. \tag{3}$$

The problem is a correct classification of solution sets given by an above equation. According to Pareto inversion concept, vector $x^* \in S$ is an optimal solution of the multiobjective problem, if all other vectors of this type produce higher value of at least one of the functions f_i. Basing on this definition, two kinds of Pareto-optimal solutions can be distinguished: strong – if there is on $x \in S$ for which $f_i(x) >= f_i(x^*)$ for all i at least one inequality is strict, and weak – if for all i $x \in S f_i(x) > f_i(x^*)$.

From the practical point of view, the main consequence of the above definitions is a possibility of simultaneous optimization of many functions over one domain, without necessity of any kind of additional operation (*e.g.*, weighting) (Kung *et al.* 1975). The given set C can be accepted against the other only if none of the changes in model parameters leads to increase of any of the optimized functitons. Additionally, during the optimization process, set of all acceptable solutions is generated, creating Pareto front. The final solution can be chosen as a set for which all functions have minimal value, or any other set from the front for which observed model parameters are in better agreement

with other, even a qualitative, information. This extends interpretational possibilities – especially for poor quality data – but in the same time eliminates any "manual" influence on final model values.

4. GLOBAL OPTIMIZATION

Complexity, multidimensionality and multimodality of many geophysical problem target functions require carefulness in result interpretation of regular method of local optimization like conjugate gradients or SIMPLEX. In the great majority of data inversion problems, the assumption that the global minimum can be obtain from any point in the line of descent is false. Moreover, solution equivalence and presence of noise make optimization even more difficult.

Advanced methods of global optimization make finding a global solution possible even for complicated multimodal deceptive target functions. Of course, the price for this functionality is an increased number of necessary computational operations (Liberti and Maculan 2006). In this kind of methods, the search over a solution space is more or less random, which leads to nonoptimal path between starting point and function minimum. Many modern methods allow limitation of this additional cost and make application of efficient parallel search possible. In this study we use Particle Swarm Optimization (Kennedy and Eberhart 1995, Poli *et al.* 2007) as a main optimization engine. PSO is a stochastic metaheuristical method combining fast problem space search with an ability of finding a solution with proper precision. The way of finding potential solution was inspired by moving swarm of insects or fish looking for food. The place where the single particle moves – a solution proposal – depends on the relation between its current position, its best solution obtained so far and the best solution obtained by the whole swarm. The so-called canonical version of algorithm update strategy is presented below:

$$\begin{aligned} & v_i \leftarrow \chi \left(v_i + U(0,\Phi_1) \otimes (p_i - x_i) + U(0,\Phi_2) \otimes (p_g - x_i) \right) , \\ & x_i \leftarrow x_i + v_i \, , \\ & \chi = \frac{2}{\Phi - 2 + \sqrt{\Phi^2 - 4\Phi}} \, , \\ & \Phi = \Phi_1 + \Phi_2 > 4 \, , \end{aligned} \tag{4}$$

where U represents uniform distribution, $\otimes$ is a componentwise multiplication, x_i represents particle position in the solution space and v_i is its velocity. p_i and p_g are the best results obtained in the previous iterations, by the particle and the whole swarm, respectively. In regular aplications, Φ is commonly set to 4.1 and $\Phi_1 = \Phi_2$. This scheme guarantees convergences without particle velocity limitations.

5. REDUCTION OF TARGET FUNCTION DIMENSIONALITY

One of the main obstacles in obtaining the joint inversion results is the problem with acquiring the parameter values in every point of computational grid. For more detailed models and consequently the more detailed grids, the dimensionality of solution can make inversion unpractical. Moreover, even if the solution can be obtained in the reasonable time, some kind of regularization has to be introduced to eliminate acceptance of chaotic, completely nongeological models (Zhdanov 2002). It is a serious problem, especially in the case of noisy data.

From mathematical point of view, this problem can be described as a minimization of misfit additionally increased by a penalty, whose value is higher for more complicated models. For example, for MT data this can be written as (Tikhonov 1963):

$$\|A(\rho) - d\| + \alpha\|\rho - \rho_a\| \rightarrow \min, \tag{5}$$

where d denotes data, A is a forward problem operator, ρ is resistivity model, ρ_a is an *a priori* resistivity model and α is a regularization coefficient defining how big is the deviation from assumed model penalization. Manipulation of this parameter makes either data or regularity more important in the inversion process, usually done through local iterative methods. The important consequences of this approach are the critical importance of starting model and usually gentle transition zones between neighboring elements of the model (*e.g.*, layers). Additionally, as it was previously mentioned, in the case of joint inversion both misfit and regularization term have to be manually scaled.

The significant reduction of these problems can be obtained with application of Sharp Boundary Interfaces concept. In this method, model is defined through series of polygons and thus radically simplified. This simplification leads to strongly reduced problem dimensionality and therefore makes SBI parameterisation very convenient for application in stochastic methods like PSO or Markov chain Monte Carlo (MCMC) (Chen *et al.* 2012).

SBI approach is based on an assumption that the maximum number of geological interfaces (*e.g.*, layers' boundaries) and the number of polygons defining points is known and set at the beginning of computations. In the subsequent steps, positions of these points and other media parameters (*e.g.*, densities, resistivities, *etc.*) are updated in the process of optimization. In this process, objects sizes can be reduced to the point of its disappearance, so elimination of an element of starting model is possible. Additionally, gradients of parameters can be also introduced and inverted to simulate facial changes. Any types of model parameter constrains are also easily applicable. If softer shapes are desirable, splines can be used instead of polygons. The general idea of simple SBI implementation is presented in Fig. 1.

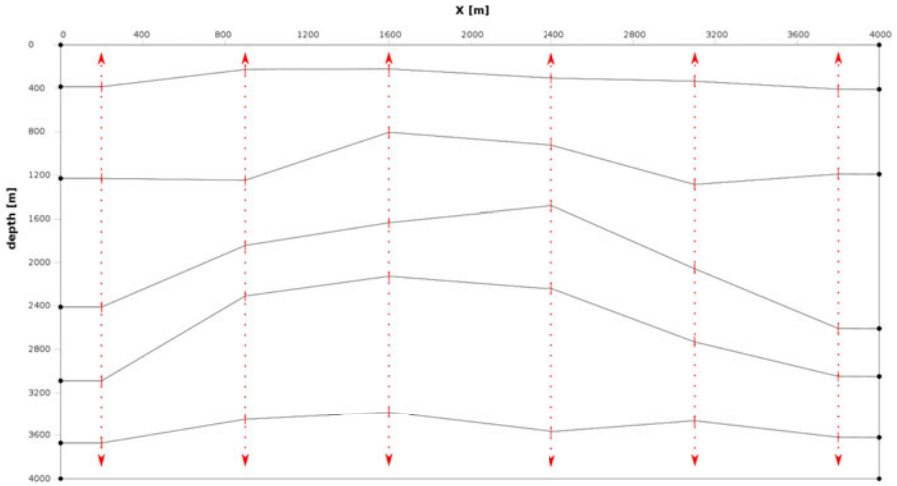

Fig. 1. Simplified SBI model example. Arrows denote direction of possible points movements. In presented case the only allowed direction is vertical.

6. IMPLEMENTATION

To obtain results for synthetic data tests, it was necessary to create fast, versatile and flexible software solution, utilizing methodology described above. Application consists of several mutually interacting modules, responsible for data input/output, model creation and rasterization, MT and gravity forward modeling, PSO inversion for SBI models and Pareto front creation.

Software was written using C language and designed for computers using operating system from Linux family. Graphical user interface was created using GTK+ library.

The first implementation issue was description of the model. As it was mentioned before, SBI approach was used. Model consists of layers, boundaries and vertices, as shown in Fig. 2. Each vertex and boundary are added to the data

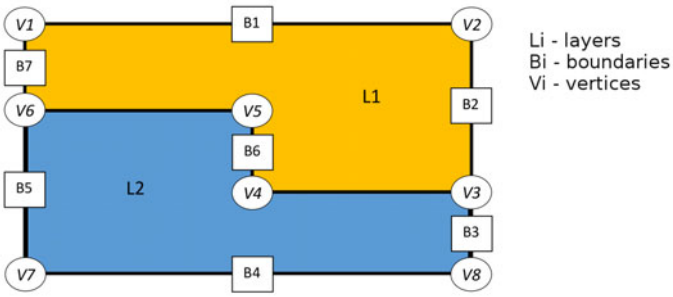

Fig. 2. Model description schema.

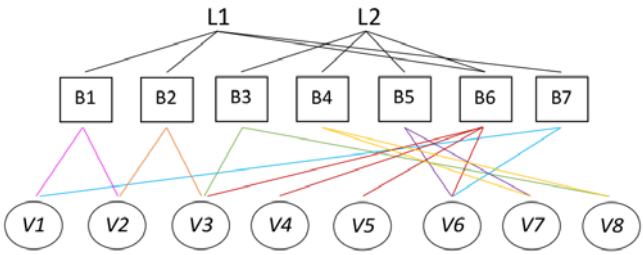

Fig. 3. Relations between objects whose describe model.

structure (list) once. Boundaries are attached to the layer by unique *id*, so two layers can have common boundaries. Relation between vertices and boundaries is the same as between boundaries and layers. Both of relations are presented in Fig. 3.

Model with this kind of description needs to be projected on calculation grid, in other words – rasterized. Rasterization is based on a simple algorithm which scheme is presented below:

1. Get first vertex of the polygon.
2. Find and mark cell comprising chosen vertex.
3. Assign line segment (made by chosen vertex and next one in order) to quadrant of the local Cartesian coordinate system (Fig. 4a):

$$\begin{aligned} &\text{quadrant I: } 0 \leq \alpha < 90, \\ &\text{quadrant II: } 90 \leq \alpha < 180, \\ &\text{quadrant III: } 180 \leq \alpha < 270, \\ &\text{quadrant IV: } 270 \leq \alpha < 360. \end{aligned} \tag{6}$$

4. Find and mark a subsequent cell. There will be three posibilities. In order to mark appropriate one, y-intercept (factor b) of the linear equation

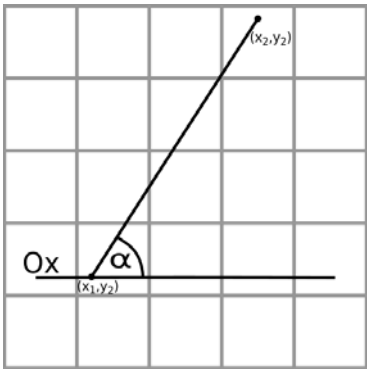

(a) Assignment of the line segment

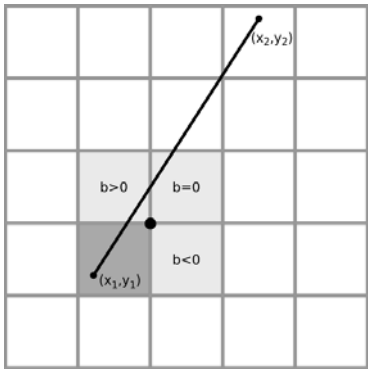

(b) Marked cell (dark grey) with three possible choises (bright grey)

Fig. 4. Scheme of line segment projection.

($y = mx + b$) must be calculated where the center of coordinate system depends on previously chosen quadrant (in the presented example center is allocated on the top-right corner of already marked cell) (Fig. 4b).

5. If the chosen cell does not contain second (last of two) vertex, go to step 4.
6. If the second vertex is the last unprocessed, one in the polygon choose it and go to step 3. Move forward as long as the marked cell does not contain last vertex (Fig. 5a).
7. Reduce to one marked cell per row for each segment line. Vertices are considered separately according to connection types, respectively for one to two, two to one, two to two, three to four, four to three; where numbers represent line segment quadrant, there is one mark per vertex and rest of possibilities implies two marks (Fig. 5b).
8. Fulfill cells beetwen marked fields (in pairs one to two) – Fig. 5c.
9. If it is not last polygon, go to the first step with next polygon.

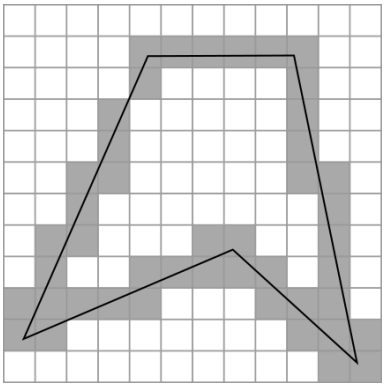

(a) Rasterized polygon

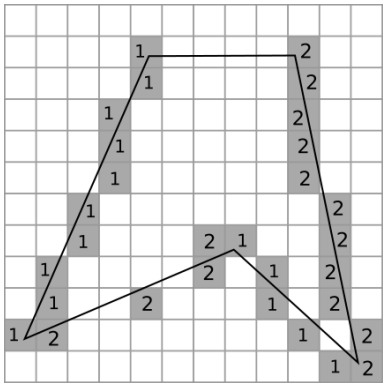

(b) Rasterized polygon after reduction

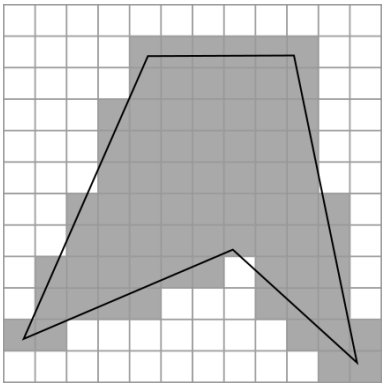

(c) Final effect

Fig. 5. Rasterization algorithm.

SBI concept assumes that the number of defined polygons is constant, so intersection of them during computation must be excluded. For this purpose two restrictions were created. The first one was implemented at the beginning as a scope in which each vertex can change their position (useful for applying seismic constraints). The second one was algorithm checking intersection between line segments (in pairs) belonging to the polygons. If line segments intersect, Eqs. 7 and 8 are true:

$$\mathrm{sign}[\det(w_{11}, w_{12}, w_{21})] \neq \mathrm{sign}[\det(w_{11}, w_{12}, w_{22})], \tag{7}$$

$$\mathrm{sign}[\det(w_{21}, w_{22}, w_{11})] \neq \mathrm{sign}[\det(w_{21}, w_{22}, w_{12})], \tag{8}$$

where w_{11}, w_{12} are vertices of first line segment, w_{21}, w_{22} are vertices of second line segment and the remaining column is filled with 1.

Forward solver for gravimetry uses superposition principle for gravity effect. Modeled gravity effect is calculated as a sum of gravity effects from all nodes of calculation grid, where each node is treated as rectangle with density value assigned. Gravity effect for single node is calculated using the following equation (Blakely 1996):

$$g = 2\gamma\rho \sum_{n=1}^{N} \frac{\beta_n}{1+\alpha_n^2} \left[\log \frac{r_{n+1}}{r_n} - \alpha_n(\Theta_{n+1} - \Theta_n) \right], \tag{9}$$

where:
γ – gravitational constant $\left(6.67 \cdot 10^{-11} \left[\frac{\mathrm{m}^3}{\mathrm{kg \cdot s}^2}\right]\right)$,
ρ – node density,
r_{n+1}, r_n – distance between measurement point and neighboring vertex of rectangle assigned to node,
Θ_{n+1}, Θ_n – angle between x axis and radius designated from measurement point to neighboring vertex,
$\alpha_n = \frac{x_{n+1}-x_n}{z_{n+1}-z_n}$,
$\beta_n = x_n - \alpha_n z_n$,
x_n, z_n – node coordinates.

For solving MT forward problem, finite difference method approximation of Helmholtz equations was used. Mentioned above equations for electric (10) and magnetic (11) polarization are presented below (Wannamaker *et al.* 1987):

$$\frac{\partial}{\partial y}\left(\frac{1}{\hat{z}}\frac{\partial E_{xs}}{\partial y}\right) + \frac{\partial}{\partial y}\left(\frac{1}{\hat{z}}\frac{\partial E_{xs}}{\partial z}\right) - \hat{y}E_{xs} = \Delta\hat{y}E_{xp}, \tag{10}$$

$$\frac{\partial}{\partial y}\left(\frac{1}{\hat{y}}\frac{\partial H_{xs}}{\partial y}\right) + \frac{\partial}{\partial y}\left(\frac{1}{\hat{y}}\frac{\partial H_{xs}}{\partial z}\right) - \hat{z}H_{xs} - \Delta\hat{y}H_{xp} = -\frac{\Delta k^2}{\hat{y}}H_{xp} + \frac{\partial}{\partial z}\left(\frac{\Delta\hat{y}}{\hat{y}}\right)E_{yp}, \tag{11}$$

where:
$\hat{y} = \sigma + i\,\omega\epsilon$ – admittance,
$\Delta\hat{y}$ – admittance's difference between the 2D inhomogeneity and its 1D host,
$\hat{z} = i\omega\mu_0$ – impedance,
$\Delta k^2 = -\Delta\hat{y}\hat{z}$, s, p – references to secondary and primary field components,
$E_{[x/y][s/p]}$ – x/y component of secondary/primary magnetic field,
$H_{x[s/p]}$ – x component of secondary/primary electric field.

Forward MT solver written in C language was based on Fortran implementation provided by Wannamaker *et al.* (1987). In this solution Dirichlet boundaries condition were applied.

All modules of created software are operate through graphical user interface (GUI) based on GTK+ library. GUI allows to input all needed parameters to run computations. User can set model and grid size, as well as initial geophysical parameters. After setting parameters, new model can be interactively created using GUI.

7. SYNTHETIC EXAMPLE

In this section, results of joint inversion for synthetic data are described. Synthetic model which simulates simplified cyclothems consequence of salt from the Zechstein formation of Polish Lowlands was used. This kind of deposits is connected with different types of mineral resources, thus their complex recognition is very important from the point of view of possible exploration opportunities. In Fig. 6 the model used for generating synthetic data is presented. For

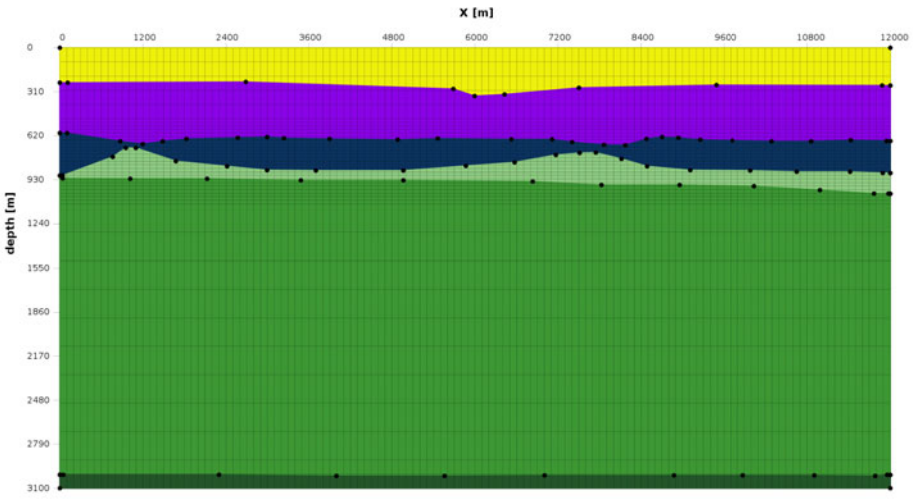

Fig. 6. Model used for generating synthetic data. See details in text.

calculation of synthetic MT data, 12 stations were located, evenly spaced, along the profile. Gravity anomaly was simulated along the same profile. Magnetotelluric curves for TM and TE mode were calculated in frequency range 10 kHz to 0.001 Hz, which allows for interpretation for both MT and AMT bands. Layers third and fourth stand for deposits of Zechstein salts and anhydrites, respectively. Resitivity of Zechstein salts and anhydrites is similar, but there is a significant difference in density. In Table 1 geophysical parameters of synthetic model are presented. In starting model for joint inversion problem both geometry and geophysical parameters of the model were perturbed. In this example PSO engine was working using 256 particles, with limit at most 1000 iterations. In Fig. 7 the geometry of starting model is presented. In this example some parts of the model were constrained to the geologically reasonable values. Vertices

Table 1

Parameters of synthetic model

No.	Density $\left[\frac{\mathrm{kg}}{\mathrm{m}^3}\right]$	Resitivity [Ωm]
1	2100	50
2	2500	10
3	1500	500
4	2700	500
5	2500	10
6	2300	1000

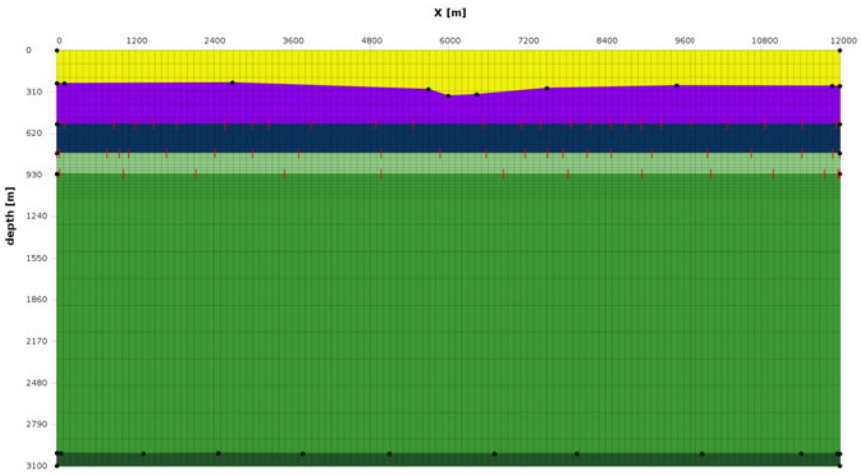

Fig. 7. Geometry of starting model. Please note that target area is reduced to 1D model.

which are able to change their position during inversion are marked with red vertical segment line, whereas unmovable vertices are marked with black dots. For tests, four different starting models were used. Their geometry was constant but diffrenet geophysical parameters were applied.

In Figs. 8–10, example fits of magnetetotelluric and gravimetry data are presented. In Fig. 11 geometry of the result model is shown.

Figure 12 presents Pareto front result, where x-axis shows fitting error for gravimetry and the y-axis for magnetotelluric. Each inversion run is illustrated

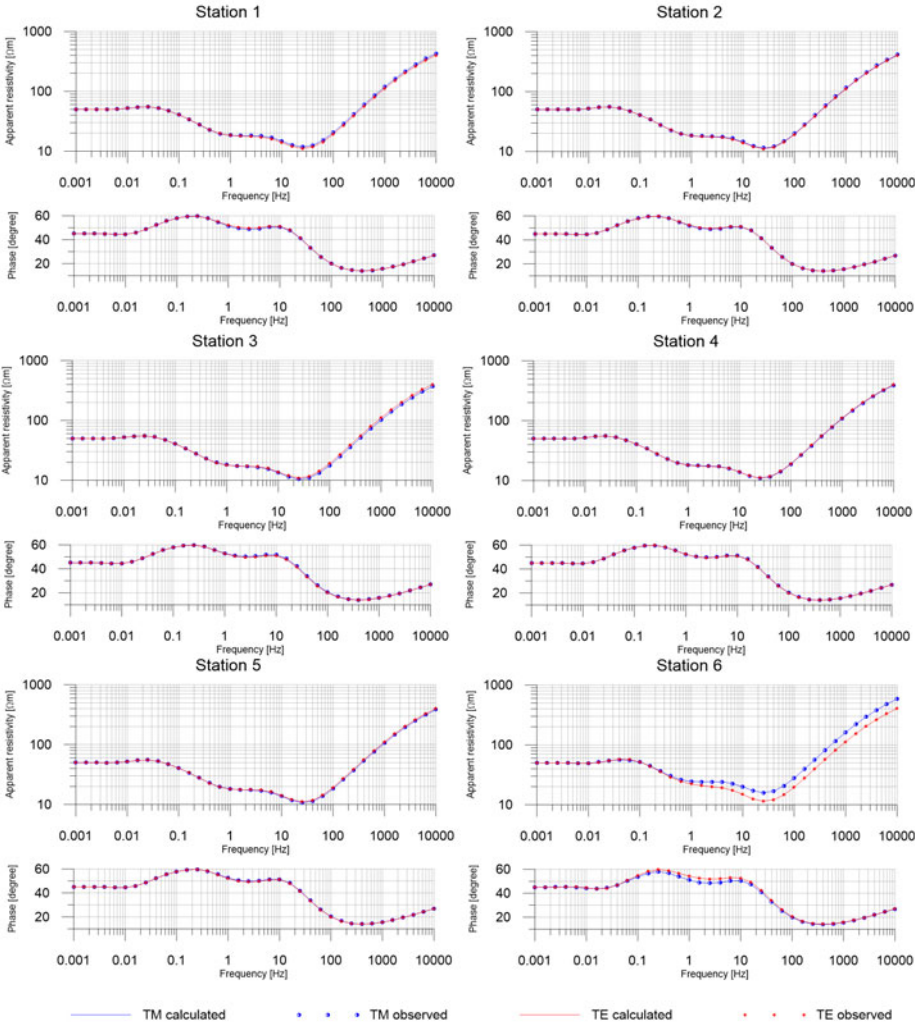

Fig. 8. Fit of calculated MT data for stations 1 – 6.

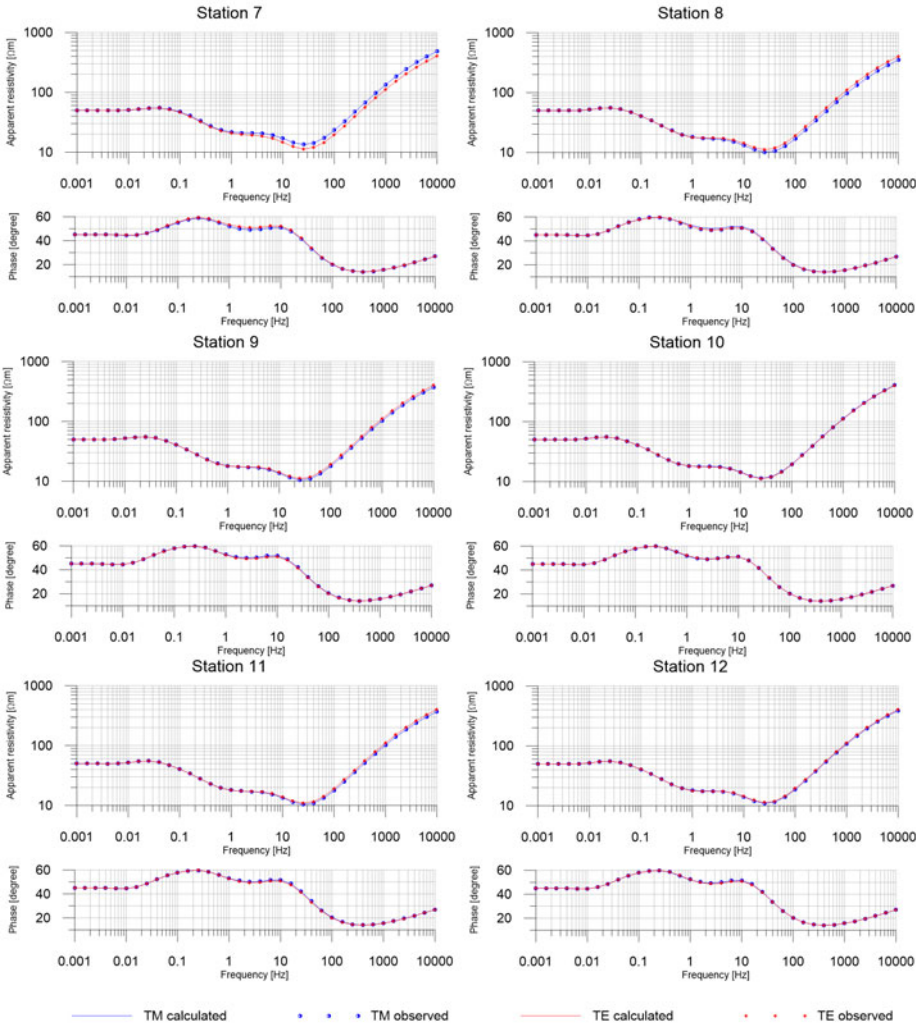

Fig. 9. Fit of calculated MT data for stations 7 – 12.

by a path marked with separate color and ends with a dot representing the final result. As the most optimal solution, the dot closest to the center of the coordinate system was chosen (Fig. 11).

8. DISCUSSION AND CONCLUSION

The proposed methodology of solving the joint inversion problem combines the advantages of Pareto inversion, global optimization and SBI. This approach is

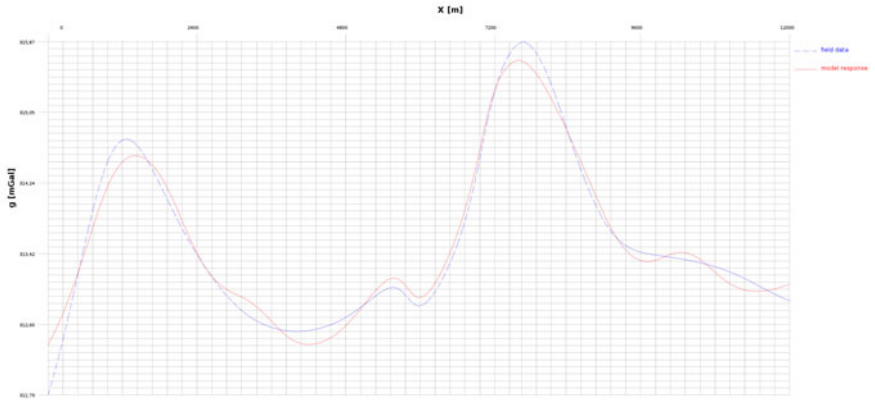

Fig. 10. Example fit of gravity data.

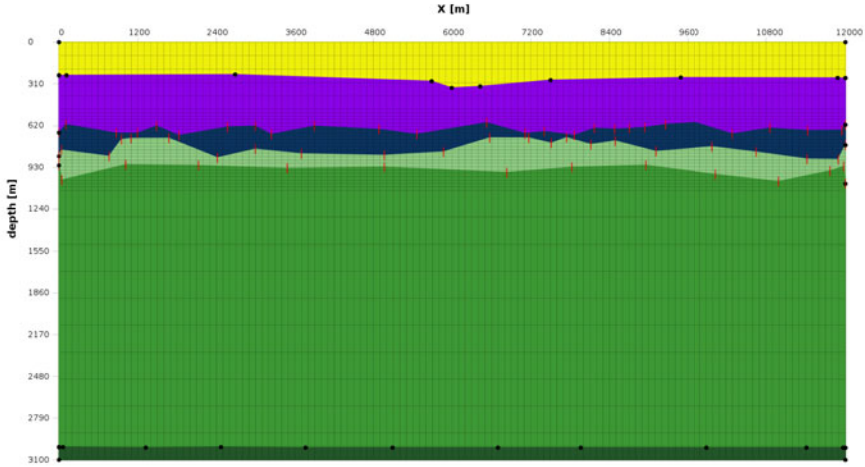

Fig. 11. Example result model.

novelty in data inversion and is very promising for geophysical investigations. In presented examples, 2D magnetotelluric and gravity data were used, but the presented solution framework can be used for any other two or more quantitative sources of information, as long as misfits between real and model data can be calculated. The results obtained for both methods are very promising. Misfits for MT data are surprisingly low, taking under consideration that MT model cannot be updated without simultaneous improvement in gravity fit. Please note that fixed interfaces between some layers make the perfect gravity fitting nearly impossible (Fig. 7). On the other hand, equivalence phenomena makes interpretation of the bottom of Zechstein complex from MT not as accurate as was demanded, especially in the right part of the profile (Fig. 11). To avoid such a situation, additional constraints for resistivities should be involved. The Pareto

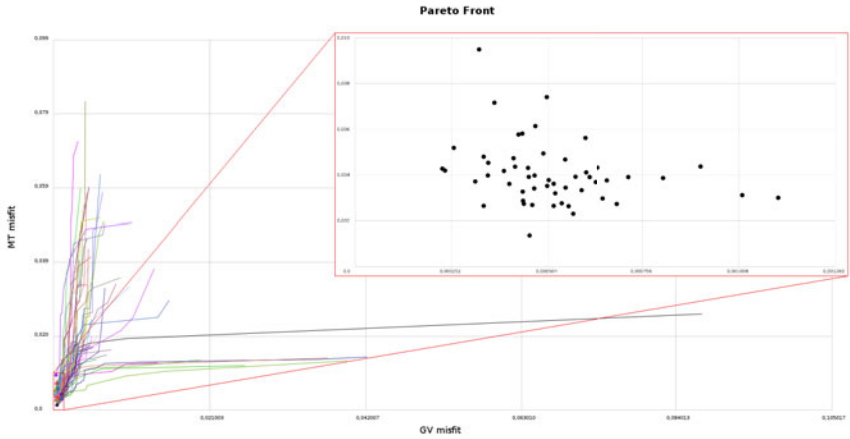

Fig. 12. Obtained Pareto front. Red frame presents details of the vicinity of Pereto optimal solution.

front presented in Fig. 12 is "blurred" because at this stage of the study no methods of deterministic local optimization are applied and the regular PSO method places a final solution in the close vicinity of the global minimum, but usually not in the exact point. This behavior is typical for many stochastic methods and – if necessary – can be easily avoid by application of local method after the final PSO iteration. Also please note that area covert by obtained front is magnified by strong zooming. Additionally, this "imperfection" of solution gives insight into shape of the final solution's basin of attraction and can be used for more or less strict uncertainty analysis in the future. The other possible areas of further studies are optimization of global solver (*e.g.*, tests for other versions of PSO or introduction of other methods like genetic algorithm) and improvement in general numerical efficiency of the code.

The presented synthetic example shows usefulness of proposed methodology in solving real-life geophysical joint inversion problems. PSO method proved its efficiency and flexibility, while SBI model provided constrained and regularized model with limited solution space dimensionality. Obtained "the best" solution shows very good misfit minimization for both data sources. Additionally, in the case of more complicated geological scenarios other results form Pareto front can be used to find a solution with better agreement with other available – either quantitative or qualitative – information. That ability makes the algorithm much more useful for interpreters who need to find the geological model that best suits to other data and conception while meeting the requirements of the correct interpretation of geophysical data.

Proposed methodology has been already used for real data from commercial investigations. Obtained results and their interpretation will be the subject of the next paper.

A c k n o w l e d g m e n t. Presented work was realized by Geopartner Ltd. and supported by Polish National Centre for Research and Development under the contract number POIG.01.04.00-12-279/13 entitled "Innovative technology of petrophysical parameters estimation of geological media using joint inversion algorithm".

R e f e r e n c e s

Abdelzaher, M., J. Nishijima, G. El-Quady, E. Aboud, O. Masoud, M. Soliman, and S. Ehara (2011), Gravity and magnetotelluric investigations to elicit the origin of Hammam Faraun hot spring, Sinai Peninsula, Egypt, *Acta Geophys.* **59**, 3, 633-656, DOI: 10.2478/s11600-011-0006-4.

Blakely, R. (1996), *Potential Theory in Gravity and Magnetic Applications*, Cambridge University Press, Cambridge.

Chen, J., G.M. Hoversten, K. Key, G. Nordquist, and W. Cumming (2012), Stochastic inversion of magnetotelluric data using a sharp boundary parameterization and application to a geothermal site, *Geophysics* **77**, 4, E265-E279, DOI: 10.1190/geo2011-0430.1.

Danek, T., M. Kochetov, and M. Slawinski (2013), Uncertainty analysis of effective elasticity tensors using quaternion-based global optimization and Monte-Carlo method, *Quart. J. Mech. Appl. Math.* **66**, 2, 253-272, DOI: 10.1093/qjmam/hbt004.

DeStefano, M. and D. Colombo (2006), Geophysical modeling through simultaneous joint inversion of seismic, gravity and magnetotelluric data. **In:** *SEG International Exhibition and 76th Annual Meeting, Workshop on Integration of Seismic and Electromagnetic Measurements*.

Fernandez Martinez, J., E. Gonzalo, J. Alvarez, H. Kuzma, and C. Menendez Perez (2010), PSO: A powerful algorithm to solve geophysical inverse problems: Application to a 1D-DC resistivity case, *J. Appl. Geophys.* **71**, 1, 13-25, DOI: 10.1016/j.jappgeo.2010.02.001.

Gauss, C. (1809), *Theoria Motus Corporum Coelestium in Sectionibus Conicis Solem Ambientium*, Kunst und Industrie Comptoir.

Jegen, M.D., R.W. Hobbs, P. Tarits, and A. Chave (2009), Joint inversion of marine magnetotelluric and gravity data incorporating seismic constraints: Preliminary results of sub-basalt imaging off the Faroe Shelf, *Earth Planet. Sci. Lett.* **282**, 1-4, 47-55, DOI: 10.1016/j.epsl.2009.02.018.

Kennedy, J., and R. Eberhart (1995), Particle swarm optimization. **In:** *Proc. IEEE International Conference on Neural Networks*, Vol. 4, 1942-1948.

Kozlovskaya, E., L. Vecsey, J. Plomerova, and T. Raita (2007), Joint inversion of multiple data types with the use of multiobjective optimization: problem formulation and application to the seismic anisotropy investigations, *Geophys. J. Int.* **171**, 2, 761-779, DOI: 10.1111/j.1365-246X.2007.03540.x.

Kung, H., F. Luccio, and F. Preparata (1975), On finding the maxima of a set of vectors, *J. ACM* **22**, 4, 469-476.

Legendre, A. (1805), *Nouvelles Methodes pour la Determination des Orbites des Cometes*, Didot Libr., Paris, 80 pp.

Liberti, L., and N. Maculan (eds.) (2006), *Global Optimization: From Theory to Implementation*, Springer Science and Business Media, New York.

Lines, L., A. Schultz, and S. Treitel (1988), Cooperative inversion of geophysical data, *Geophysics* **53**, 1, 8-20, DOI: 10.1190/1.1442403.

Mehanee, S., and M. Zhdanov (2002), Two-dimensional magnetotelluric inversion of blocky geoelectrical structures, *J. Geophys. Res.* **107**, B4, 2156-2202, DOI: 10.1029/2001JB000191.

Poli, R., J. Kennedy, and T. Blackwell (2007), Particle swarm optimization. An overview, *Swarm Intell.* **1**, 1, 33-57, DOI: 10.1007/s11721-007-0002-0.

Sen, M., and P. Stoffa (1995), *Global Optimization Methods in Geophysical Inversion*, Elsevier, Amsterdam.

Smith, T., M. Hoversten, E. Gasperikova, and F. Morrison (1999), Sharp boundary inversion of 2D magnetotelluric data, *Geophys. Prospect.* **47**, 4, 469-486, DOI: 10.1046/j.1365-2478.1999.00145.x.

Tikhonov, A. (1963), Regularization of incorrectly posed problems, *Dokl. Akad. Nauk SSSR* **4**, 1624-1627.

Vozoff, K., and D. Jupp (1975), Joint inversion of geophysical data, *Geophys. J. Int.* **42**, 3, 977-991, DOI: 10.1111/j.1365-246X.1975.tb06462.x.

Wannamaker, P., J. Stodt, and L. Rijo (1987), A stable finite element solution for two-dimensional magnetotelluric modelling, *Geophys. J. Int.* **88**, 1, 277-296, DOI: 10.1111/j.1365-246X.1987.tb01380.x.

Zhdanov, M. (2002), *Geophysical Inverse Theory and Regularization Problems*, Elsevier, Amsterdam.

Received 18 January 2016
Accepted 18 February 2016